



Degree Project in Applied Physics

Second cycle, 30 credits

Effects of Glucose Availability on Mitochondrial Dynamics

Quantitative Live-cell Analysis in MDCK II Cells

ANDREA SÖDERBERG

Effects of Glucose Availability on Mitochondrial Dynamics

Quantitative Live-cell Analysis in MDCK II Cells

ANDREA SÖDERBERG

Master's Programme, Engineering Physics, 120 credits

Date: May 29, 2026

Supervisor: Steven Edwards

Examiner: Hjalmar Brismar

School of Engineering Sciences

Host organization: SciLifeLab

Swedish title: Effekter av glukostillgång på mitokondriedynamik

Swedish subtitle: Kvantitativ analys av levande MDCK II-celler

Abstract

Mitochondria are dynamic organelles which play a central role in the cellular energy metabolism and intracellular signaling. Changes in mitochondrial movement and organisation have been linked to metabolic states, cellular stress and disease development. The purpose of this thesis was to investigate how different glucose concentrations affect mitochondrial movement in living MDCK II cells, as well as to evaluate the use of automated analysis methods for quantification of mitochondrial dynamics.

Living MDCK II cells expressing mitochondria-targeted GFP were imaged with fluorescence microscopy under three different glucose conditions: high glucose, low glucose and a physiological baseline. Mitochondrial trajectories were extracted and analysed using the Python-based framework Nellie together with a custom Python analysis pipeline. The mitochondrial movement patterns were characterised by calculating the mean squared displacement (MSD), anomalous diffusion exponent (α), velocity, step displacement and confinement ratio. The results were compared with an independent AI-based pipeline, generated with the large language model Claude.

The results showed that mitochondrial motion was predominantly confined in all glucose concentrations, with α -values below 1 for the large majority of trajectories. High glucose concentration showed somewhat elevated values for MSD, velocity and step displacement when compared with values for low and baseline concentrations of glucose, but the statistical differences were generally small. The comparison between the Nellie-based pipeline and the AI-based pipeline revealed similar overarching trends between glucose conditions, although there were differences in absolute values.

The thesis showed that automated motion analysis can be used to quantify mitochondrial motion in living cells, while changes in glucose concentration produced only moderate effects on mitochondrial movement under the experimental conditions used in this project.

Keywords

Mitochondria, Fluorescence microscopy, Mean squared displacement, MDCK II, Glucose metabolism, Nellie, Trajectory analysis

Sammanfattning

Mitokondrier är dynamiska organeller som spelar en central roll i cellernas energimetabolism och intracellulära signalering. Förändringar i mitokondriernas rörelse och organisation har kopplats till metabola tillstånd, cellulär stress och sjukdomsutveckling. Syftet med detta examensarbete var att undersöka hur olika glukoskoncentrationer påverkar mitokondriell rörelse i levande MDCK II-celler, samt att utvärdera användningen av automatiserade analysmetoder för kvantifiering av mitokondriell dynamik.

Levande MDCK II-celler som uttryckte mitokondrie-riktat GFP avbildades med fluorescensmikroskopi under tre olika glukoskoncentrationer: hög glukos, låg glukos och ett fysiologiskt bastillstånd. Mitokondriella rörelsebanor extraherades med det Python-baserade analysverktyget Nellie, och analyserades med ett skräddarsytt Python-program. Mitokondriernas rörelsemönster karaktäriserades genom beräkning av mean squared displacement (MSD), anomal diffusionsexponent (alpha), hastighet, stegförflyttning och confinement ratio. Resultatet jämfördes med en separat AI-baserad analysmetod, genererad med hjälp av språkmodellen Claude.

Resultaten visade att mitokondriell rörelse uppvisade huvudsakligen konfinerad rörelse i samtliga glukoskoncentrationer, med alpha-värden under 1 för den stora majoriteten av rörelsebanor. Hög glukoskoncentration visade något förhöjda värden för MSD, hastighet och stegförflyttning jämfört med låg- och baskoncentration av glukos, men de statistiska skillnaderna mellan glukoskoncentrationer var generellt små. Jämförelsen mellan den Nellie-baserade analysmetoden och den AI-baserade analysmetoden visade liknande övergripande trender mellan glukosförhållandena, trots skillnader i absoluta värden.

Examensarbetet visar att automatiserad rörelseanalys kan användas för att kvantifiera mitokondriell rörelse i levande celler, samt att förändringar i glukostillgång endast gav begränsade effekter på mitokondriell rörelse under de använda experimentella förhållandena.

Nyckelord

Mitokondrier, Fluorescensmikroskopi, Mean squared displacement, MDCK II, Glukosmetabolism, Nellie, Trajektorieanalys

Acknowledgments

I would like to sincerely thank Professor Hjalmar Brismar for the opportunity to conduct my master's thesis project within the Brismar research group, and for valuable feedback throughout the project.

Thank you to my supervisor, Steven Edwards, for guidance and support throughout the thesis, particularly regarding microscopy imaging.

I would also like to thank the entire Brismar research group, for creating a welcoming and supportive research environment.

And to my friends and family: thank you for your unconditional support throughout these five years. I would not have managed it without you.

Stockholm, May 2026

Andrea Söderberg

Contents

1	Introduction	1
1.1	Background	1
1.2	Purpose	2
1.3	Goals	2
1.4	Research Methodology	3
1.5	Delimitations	3
1.6	Structure of the Thesis	4
2	Background	5
2.1	Structure and Function of Mitochondria	5
2.2	Fusion, Fission and Network Organisation	6
2.3	Mitochondrial Movement and Intracellular Transport	7
2.4	Cellular Energy Metabolism	8
2.5	Metabolic Flexibility and the Role of Glucose Availability	9
2.6	Links Between Metabolism, Morphology and Movement	9
2.7	MDCK Cells	10
2.8	Live Cell Imaging of Mitochondria	10
2.9	Mean Squared Displacement Analysis	11
2.10	Nellie Framework	12
2.11	Statistical comparison of groups	13
3	Method	14
3.1	Cell Culturing	14
3.1.1	Cell Line and Culture Medium	14
3.1.2	Cell Thawing and Passaging	15
3.1.3	Imaging Preparation	15
3.2	Glucose Treatment	15
3.3	Microscopy	17
3.4	Image Processing and Mitochondrial Tracking	18

3.5	MSD and Trajectory Analysis	19
3.6	AI-based Pipeline	20
4	Results	22
4.1	Overview of Dataset	22
4.2	Mitochondrial Movement Assessed by MSD Analysis	24
4.3	Motion Classification	25
4.4	Velocity, Confinement and Displacement	28
4.5	Statistical Comparison	30
4.6	Nellie and Claude AI Pipeline Comparison	30
5	Discussion	33
5.1	Predominantly Confined Mitochondrial Motion	33
5.2	Effects of Glucose	34
5.3	Methodological Limitations	35
5.3.1	Imaging Limitations	36
5.3.2	Biological Variability	36
5.3.3	Computational Limitations	37
5.4	Computational Pipeline Comparison	37
5.5	Evaluation of Nellie	38
6	Conclusion	40
6.1	Conclusion	40
6.2	Future Work	41
	References	43
A	Cell Culture	47
A.1	Materials	47
A.2	Routine Subculturing	48
A.3	Seeding Protocol	48
B	Glucose Medium	50
B.1	Glucose Concentrations	50
B.2	Inorganic Salt Composition	50
B.3	Amino Acid Composition	51
B.4	Vitamin Composition	51
C	MSD validation	53

List of Figures

4.1	Overview of mitochondrial image analysis workflow.	23
4.2	MSD curves of mitochondrial trajectories under differing glucose conditions.	24
4.3	Distribution of anomalous diffusion exponents (α) across glucose conditions.	26
4.4	Log-log MSD plots across glucose conditions.	27
C.1	Qualitative validation of MSD analysis.	54

List of Tables

3.1	Glucose concentrations used for the different culture conditions.	16
3.2	Composition of inorganic salts in culture medium.	16
3.3	Additional organic components present in the culture medium.	16
3.4	Microscopy acquisition settings used for time-lapse imaging of mitochondria.	18
4.1	Overview of analysed mitochondrial trajectory dataset.	23
4.2	MSD values across glucose conditions.	25
4.3	Summary of α values and motion classifications.	25
4.4	Mitochondrial motion metrics per biological replicate.	29
4.5	Summary of mitochondrial motion descriptors across glucose conditions.	30
4.6	Pairwise p-values between glucose conditions for MSD- derived metrics.	30
4.7	Comparison of Nellie and Claude pipelines.	32
B.1	Glucose concentrations used for the different culture conditions.	50
B.2	Composition of inorganic salts in culture medium.	51
B.3	Amino acid composition of the culture medium.	51
B.4	Vitamin composition of the culture medium.	52

List of acronyms and abbreviations

EAMSD	ensemble-averaged mean squared displacement
EMEM	Eagle's minimum essential medium
FBS	fetal bovine serum
GFP	green fluorescent protein
MDCK	Madin-Darby canine kidney
MEM	minimum essential medium
MSD	mean squared displacement
PBS	phosphate-buffered saline
RH	relative humidity
ROI	region of interest
ROS	reactive oxygen species
TAMSD	time-averaged mean squared displacement
TEAMSD	time-ensemble-averaged mean squared displacement

Chapter 1

Introduction

1.1 Background

Mitochondria are membrane-bound organelles which are involved in several essential cellular processes, including ATP-production, calcium regulation and apoptosis. In addition to their central role in cellular metabolism, mitochondria are highly dynamic structures, capable of continuous movement and structural rearrangement within the intracellular environment [1].

Mitochondrial dynamics and morphology are highly responsive to cellular state and metabolic conditions. Mitochondria continuously undergo fusion and fission events, and form complex intracellular networks whose organisation can change substantially in response to physiological stress or altered metabolic demands [2].

Dysfunction of mitochondrial metabolism and dynamics have been associated with several pathological conditions, including neurodegenerative disease, metabolic disorders, aging and cancer [2], [3]. Alterations in mitochondrial morphology and intracellular transport have therefore become an important area of biomedical research.

Cellular metabolic state strongly influences mitochondrial function and organisation [4]. Cancer cells and other rapidly proliferating cells frequently exhibit increased glycolytic activity compared to quiescent cells [5], suggesting that glucose availability may influence mitochondrial behaviour and intracellular transport dynamics.

Mitochondrial movement is an active, energy-dependent process driven by motor proteins along the cytoskeleton. Because glucose availability influences cellular metabolism and ATP production, changes in glucose availability may affect mitochondrial motility. In high glucose conditions, increased

ATP availability may enhance motor-driven transport and therefore increase mitochondrial movement. It was therefore hypothesised that a higher glucose concentration may give rise to increased motility in mitochondria.

Despite the increasing importance of mitochondrial dynamics in both cell biology and disease research, quantitative analysis of mitochondrial motion remains challenging due to the structural complexity and dynamic behaviour of mitochondrial networks. Automated computational approaches for motion analysis may therefore provide valuable tools for investigating intracellular mitochondrial dynamics in live-cell fluorescence microscopy data. Understanding how mitochondrial motion changes under different metabolic conditions may also contribute to improved understanding of intracellular mitochondrial behaviour and the development of computational approaches for analysing mitochondrial dynamics.

1.2 Purpose

The purpose of this thesis project was to investigate mitochondrial dynamics in living Madin-Darby canine kidney (MDCK) II cells under different glucose conditions using fluorescence microscopy and computational trajectory analysis. Quantitative characterisation of mitochondrial motion in live cells remains challenging due to their complex morphology and variable intracellular behaviour; this thesis therefore aimed to apply and evaluate computational approaches for extracting and analysing mitochondrial trajectories from time lapse microscopy data.

1.3 Goals

More specifically, the goals of this thesis were to quantify mitochondrial motion using mean squared displacement (MSD) analysis, characterise mitochondrial movement under different glucose conditions using parameters such as anomalous diffusion exponent, velocity, step displacement and confinement ratio, and assess the performance of the Nellie tracking framework [6] by comparing its output with outputs obtained from an independent AI-based computational analysis pipeline.

1.4 Research Methodology

This thesis combined live-cell fluorescence microscopy with computational image analysis to investigate mitochondrial dynamics in MDCK II cells. Mitochondria were visualised using mitochondria-targeted green fluorescent protein (GFP) and recorded over time using time lapses under different glucose conditions. The resulting time lapses were processed using the Nellie tracking framework to extract mitochondrial trajectories.

Extracted trajectories were subsequently analysed using a custom Python-based workflow to compute quantitative descriptors of mitochondrial motion, including MSD, anomalous diffusion exponent, velocity, step displacement and confinement ratio. Additionally, results obtained from the Nellie-based pipeline were compared with those obtained using an independent AI-based pipeline in order to evaluate consistency between methods.

1.5 Delimitations

This thesis had several delimitations. The project was restricted to MDCK II cells, meaning that findings may not be directly applicable to other cell types. Mitochondrial dynamics was also analysed only under selected glucose conditions, high, low and baseline conditions, and therefore do not capture the full range of possible states.

The analysis was further limited to two-dimensional fluorescence microscopy time lapses, which do not capture potential three-dimensional aspects of mitochondrial movement. Due to computational constraints associated with trajectory extraction and processing, as well as time constraints, only a limited number of time lapses were included in the analysis, and only one cell per recording was selected for quantitative evaluation.

Additionally, the project focused exclusively on trajectory-based quantification of mitochondrial motion and did not investigate underlying molecular mechanisms governing mitochondrial transport, such as motor protein activity or cytoskeletal interactions. Finally, although two computational analysis approaches were compared (the Nellie-based pipeline and an AI-based pipeline), the comparison was limited to these specific methods and does not represent an exhaustive evaluation of all available mitochondrial tracking frameworks.

1.6 Structure of the Thesis

This thesis is structured as follows: Chapter two presents the theoretical background regarding mitochondrial dynamics, fluorescence microscopy and computational analysis of intracellular motion. Chapter three describes the experimental design and computational methods used for image acquisition, trajectory extraction and motion analysis. Chapter four presents the results obtained from the analysis of mitochondrial dynamics under different glucose conditions. Chapter five discusses the biological interpretation of the findings, methodological limitations, and a comparison between computational analysis pipelines. Chapter six, finally, provides the overall conclusion of the study and outlines directions for future work.

Chapter 2

Background

This chapter presents the biological, experimental and computational background relevant to the present study. Section 2.1 introduces the structure and function of mitochondria, followed by Section 2.2 and Section 2.3, which describe mitochondrial dynamics, intracellular transport and network organisation. Section 2.4 and Section 2.5 provide an overview of cellular energy metabolism and the effects of altered glucose availability on mitochondrial function. Section 2.6 discusses the relationship between metabolism, mitochondrial morphology and motility.

Section 2.7 introduces the MDCK II cell model used throughout the project, while Section 2.8 describes the principles of live-cell fluorescence imaging used to visualise mitochondrial dynamics. Section 2.9 presents the theoretical basis of MSD analysis and anomalous diffusion. Finally, Section 2.10 introduces the Nellie framework and the statistical methods used for quantitative comparison between experimental conditions.

2.1 Structure and Function of Mitochondria

Mitochondria are double-membrane organelles present in eukaryotic cells. They have an important role in ATP production, and are therefore often referred to as the “powerhouse of the cell”. Mitochondria are also unique among other organelles, as they contain their own DNA [1].

Mitochondria are built up of an outer and an inner mitochondrial membrane. The membranes are separated by an intermembrane space, and the interior of the mitochondria is called the matrix. The inner membrane is folded numerous times into folds, called cristae. The cristae increase the surface area of the inner membrane, which increases the area where

oxidative phosphorylation can occur. The matrix contains enzymes necessary for oxidative metabolism. Together with the inner mitochondrial membrane, the matrix is mostly responsible for the mitochondrial functions [1].

The most important function of the mitochondria is the ATP production through oxidative phosphorylation. NADH and FADH₂ function as electron donors in the electron transport chain in the inner mitochondrial membrane. When electrons are transferred through this chain, protons are pushed over the inner membrane, creating an electrochemical proton gradient across the membrane. This gradient drives the ATP synthesis. Through this process, mitochondria produces approximately 32 to 34 ATP molecules. This makes oxidative phosphorylation the dominant source of ATP in most aerobic cells [1].

Except for their role in energy production, mitochondria are involved in several other important cellular processes. They play a central part in the regulation of programmed cell death, apoptosis, by releasing pro-apoptotic factors from the mitochondria intermembrane space. Mitochondria also aid the regulation of calcium concentration in the cells, which is important for different signaling processes. The mitochondria are also an important source of reactive oxygen species (ROS), which are created as byproducts of the electron transport chain. Although high levels of ROS can be harmful to the cell, these molecules also function as important signaling molecules in several metabolic and cellular processes. Through these functions, mitochondria are closely connected to the cell's overall metabolism and physiological condition [1].

2.2 Fusion, Fission and Network Organisation

Mitochondria are not static organelles; they show a high degree of dynamics in living cells. They continuously change shape, size and organization through processes where mitochondria continuously divide or fuse together. As a result of these processes, mitochondria often form complex networks in the cell, rather than existing as completely separate organelles. This dynamic organization allows the cell to adjust the mitochondrial structure and distribution in response to changes in energy demand and metabolic condition [2]. These networks are continuously changing through fusion and fission. Their morphology can change between tubular, hyperfused or fragmented to fit to the metabolic state of the cell [7].

Mitochondrial fusion implies two mitochondria merging together and forming a larger unit. This process allows for an exchange of metabolites, proteins and mitochondrial DNA. Fusion is seen as important to maintain the mitochondrial functions through enabling an exchange of components between different mitochondria, thereby counteracting local damage or functional defects [7]. Fusion also contributes to the formation of more cohesive mitochondrial networks, which can improve the energy distribution of the cell. Fusion has been associated with increased energy efficiency, improved stress resistance and regulation of cellular signalling pathways [2].

Mitochondrial fission is the opposite process, where mitochondria are divided into two smaller organelles. This process is important for regulating the number of mitochondria, ensuring proper distribution of mitochondria in the cell as well as removing damaged mitochondrial components through quality control mechanisms, such as mitophagy [7], [8].

The balance between fusion and fission largely decides the overall morphology of the mitochondria and their network structure in the cell. Changes in this balance can lead to more fragmented mitochondria or more cohesive networks, which in turn might affect the mitochondrial function and cellular metabolism [7].

2.3 Mitochondrial Movement and Intracellular Transport

Mitochondria are not solely dynamic in their shape, but can also actively move within the cell. This movement is important to ensure that mitochondria are distributed to areas in the cell where energy needs are high. By moving to specific regions in the cell, the mitochondria contribute to maintaining local ATP production as well as regulating different signaling processes. The dynamic nature of mitochondria in the cells is governed and maintained stable by the balance of several processes: synthesizing of new mitochondria, the removal of damaged or dysfunctional mitochondria, fusion and fission as well as motility [8], [9]. The subcellular distribution of mitochondria is important, as they locally regulate ATP and calcium concentrations, which support processes demanding energy [3].

Mitochondrial movement occurs along the cytoskeleton of the cell, primarily along microtubuli, where motor proteins can perform long distance transport of mitochondria [3], [9], [10]. This transport makes movement of mitochondria to areas which have a high energy demand possible [10]. At

the same time, mitochondria can also exhibit local, shorter range movement in the cytoplasm by actin-based transport, contributing to a more fine tuned distribution within the cell [8], [9]. The movement of mitochondria along the cytoskeleton contributes to proper distribution in the cell, and is functionally important for cellular energy balance [10].

Although mechanisms for active transport of mitochondria have been identified, the relative contribution of random versus directed motion is still an area of interest. In some studies, mitochondrial movement has been described as stochastic, meaning that it largely can be likened to random diffusion. At the same time, other observations have indicated that the movement may be more organized and be affected by cellular factors, such as energy demand, cytoskeletal organization and metabolic condition. Experimental studies have shown that mitochondrial motion can include both diffusive movement and intermittent directed transport driven by motor proteins [11]. To determine if mitochondrial movement is mainly random or directed is therefore an important question within the study of mitochondrial dynamics [9]

2.4 Cellular Energy Metabolism

Cells generate energy through several metabolic processes, where glucose often functions as a central energy source. The first step of the cellular respiration is the glycolysis, which occurs in the cytosol. During this process, one glucose molecule is broken down into two pyruvate molecules through a series of enzymatic reactions, producing a net gain of two ATP molecules and two NADH molecules. This process does not require oxygen, and can therefore contribute to the energy supply of the cell, even during conditions where mitochondrial respiration is limited [4].

In conditions with oxygen, the pyruvate molecules that are created during the glycolysis are transported into the mitochondria where they are converted into acetyl-CoA, and then enter the citric acid cycle. In this cycle, acetyl groups are oxidised and the energy is stored in reducing coenzymes, mainly NADH and FADH₂. These molecules then work like electron donors to the electron transport chain in the inner mitochondrial membrane. Electron transport drives proton pumps across the inner mitochondrial membrane, which generates an electrochemical gradient. This gradient drives the ATP synthesis through oxidative phosphorylation. This process produces the majority of cellular ATP, approximately 32 to 34 ATP molecules, under aerobic conditions [1].

2.5 Metabolic Flexibility and the Role of Glucose Availability

Cells have a high degree of metabolic flexibility, which means that they can adapt their energy producing pathways depending on the availability of nutrients and energy demand. Glucose is one of the most important energy sources for many cell types, and changes in glucose availability can therefore lead to changes in the cell's metabolic activity. When glucose availability is high, glycolysis can contribute more significantly to ATP production, while mitochondrial respiration is particularly important for efficient ATP production under aerobic conditions [4], [5].

Changes in glucose metabolism can affect the mitochondrial function and organisation in the cell. Metabolic signals can regulate mitochondrial dynamics, including processes such as fusion, fission and changes in mitochondrial networks. These changes can in turn affect how mitochondria are distributed and function in the cell [3], [11].

2.6 Links Between Metabolism, Morphology and Movement

Mitochondria are central for the cell's energy metabolism. Their structure and functions are closely coupled to the cell's metabolic state. Changes in metabolic activity can affect the mitochondrial organisation and morphology. For example, changes in energy demand or nutrient availability can affect the balance between mitochondrial fusion and fission, which in turn leads to changes in mitochondrial network structure. These dynamic changes are considered an important mechanism through which cells can adapt their energy production to varying metabolic conditions [2], [3].

Changes in mitochondrial structure and network organisation can also affect how they are distributed and move within the cell. Mitochondria can be transported to areas where the energy demand is high, which means that their positioning in the cell might be functionally meaningful. Earlier studies have suggested that mitochondrial dynamics, including movement and network creation, can be regulated by cellular signals which are connected to metabolism and energy status [3], [9].

Because mitochondrial dynamics are affected by the cell's metabolic condition, it is reasonable to investigate whether changes in energy metabolism

also could affect the mitochondrial movement patterns. Variations in glucose availability can change how cells produce energy and therefore potentially influence the mitochondria activity, organisation and movement within the cell. Studies of mitochondrial movement under different metabolic conditions can therefore contribute to a better understanding of how cells adjust their energy supply to changing physiological environments [3].

2.7 MDCK Cells

MDCK (Madin-Darby Canine Kidney) cells are an epithelial cell line, originating from canine kidney tubule tissue. They are widely used as a model system for studying epithelial cell biology [12]. MDCK cells exhibit characteristic epithelial properties, including apico-basolateral polarity, the formation of tight monolayers, and organized intercellular structure. These features make them a well-established model for studying spatial organisation and intracellular transport processes in polarized cells [12], [13].

There are several different strains of MDCK with differing physiological and morphological properties, including the parental strain NBL-2, and subtypes such as MDCK I and MDCK II. MDCK II cells are derived from higher passage parental MDCK cultures, and are larger and taller in comparison to MDCK I cells. MDCK II are one of the most commonly used epithelial subtypes in cell biology research, and are recommended for researchers who have not previously worked with MDCK cells [12].

2.8 Live Cell Imaging of Mitochondria

Live cell imaging is a method used to observe cellular processes in real time in living cells, enabling quantitative analysis of mitochondrial dynamics. To understand mitochondrial dynamics, it is important to study movement and interactions when the organelles are intact and metabolically active. By imaging mitochondria in living cells, it is possible to study their positioning, movement patterns and network organisation under differing experimental conditions [10].

Fluorescence microscopy is commonly used in live cell imaging to selectively mark and visualise biomolecules in cells. This is achieved using fluorescent probes. Fluorophores absorb light at specific excitation wavelengths, and then emit light at longer wavelengths. Once excited, the fluorophore is promoted to an excited electronic state. When it is returned

to its original state, it emits a photon of lower energy. The signal that is emitted is usually weaker than the excitation light, which creates a need for separation of the two to avoid signal contamination. By using an excitation filter, a dichroic mirror and an emission filter, these signals are separated. These components together ensure that only the emitted fluorescence reaches the detector by selectively transmitting and reflecting specific wavelength ranges. The process of image acquisition starts when light from an excitation source, for example an LED or laser, is directed through an excitation filter that selects an appropriate wavelength range. The filtered excitation light is reflected by a dichroic mirror and is focused onto the sample through an objective lens. The fluorophores in the sample absorb this light and then emit fluorescence at longer wavelengths. The emitted light is collected by the objective lens, transmitted through the dichroic mirror and an emission filter, which removes remaining excitation light, and finally recorded by a detector, such as a camera[14]. This allows mitochondrial structures and movements to be tracked over time in living cells without fixation or cell death. This approach provides sufficient contrast and spatial resolution for tracking mitochondrial dynamics in cellular environments[10].

In this project, the fluorescent protein used was GFP (Green Fluorescent Protein) targeted to mitochondria. GFP is fused to a mitochondrial targeting sequence, which specifically directs the protein to the mitochondria, and enables visualization of mitochondrial structure and dynamics in living cells[15].

Time lapses are created in live cell imaging by taking sequential images of the same cells during a defined time period, enabling analysis of dynamic processes. During time lapse acquisition, care has to be taken to minimise phototoxicity and photobleaching. These can harm cells or potentially affect mitochondrial behavior; mitochondria may reduce their motility when phototoxicity occurs. By optimising illumination intensity, exposure time and imaging frequency, these effects can be reduced[10].

2.9 Mean Squared Displacement Analysis

MSD analysis is a quantitative method used to describe particle motion by measuring how far a particle moves over time [16]. By analysing the change in position of a particle at different points in time, trajectories for individual particles can be reconstructed and their movement characteristics can be determined. The most commonly used formulation is the time-averaged mean squared displacement (TAMSD), which is calculated along individual

trajectories. ensemble-averaged mean squared displacement (EAMSD) can also be computed across multiple particles, and both approaches may be combined in time-ensemble-averaged mean squared displacement (TEAMSD) when required [17].

MSD is calculated by taking the square of the displacement of a particle between two timepoints, and then taking the average over all time intervals in a tracking series (Equation (2.1)). This gives a function which describes how the average squared displacement changes as a function of lag time τ , where $\mathbf{r}(t)$ describes the particle position at time t . MSD averages all position pairs in a trajectory, indicated by the angular brackets. Ensemble averaging over several particles can be used to improve statistical robustness [16].

$$\text{MSD}(\tau) = \langle |\mathbf{r}(t + \tau) - \mathbf{r}(t)|^2 \rangle \quad (2.1)$$

MSD follows a power-law relationship (Equation (2.2)).

$$\text{MSD}(\tau) \propto \tau^\alpha \quad (2.2)$$

This scaling relation describes how displacement grows over time and is commonly used to characterize anomalous diffusion [11]. The exponent α describes the scaling behavior of the motion, and is obtained from the slope in a log-log plot of MSD versus time. Different types of motion can be distinguished based on the value of α :

- **Brownian motion:** MSD increases linearly with time ($\alpha = 1$), indicating a random motion without direction.
- **Directed motion:** MSD increases faster than linearly with time ($\alpha > 1$), indicating directed or active movement.
- **Confined motion:** MSD increases slower than linearly and may plateau over time ($\alpha < 1$), indicating limited or confined movement.
- **Ballistic motion:** Represents the limiting case of fully directed motion ($\alpha = 2$) [16].

2.10 Nellie Framework

Analysis of organelles in living cells often generate large amounts of data from time lapse microscopy. Manual analysis of these datasets are both time consuming and difficult to reproduce, especially when many organelles need to

be identified and tracked over time. Therefore, automated image analysis tools are needed to segment, track and extract quantitative traits from microscopy images [6].

Other tools used to segment and track intracellular structures are more time consuming and rely somewhat on manual techniques, and are difficult to use when working with large or spatially 3D data. Other automated tools usually have some issues regarding matters such as complexity and variability of the biological imaging data used, or poor accuracy in segmentation if the objects in the images are small or dim [6].

Nellie is an automated image analysis framework developed to study the dynamics of organelles in two and three dimensional microscopy images. The Nellie software first utilizes multiscale preprocessing to enhance structures of differing sizes, which improves the visibility of fine and large features while suppressing noise. The image is then segmented to identify organelles, which are further divided into smaller structural components, such as branches and junctions. The subcomponents are converted into motion capture markers, or mocaps. The mocaps are matched between consecutive frames using pattern recognition, which creates links between frames and allows tracking over time. Nellie applies temporal interpolation algorithms which enables subvoxel tracking, or precision smaller than a pixel. This improves tracking accuracy beyond image resolution [6].

The Nellie pipeline is run using a Napari GUI [18]. The user loads their image data, which can be either 2D or 3D, single frame or a time lapse. The user can then confirm, or adjust if needed, metadata such as dimensions and resolution. Then the user can click to run the pipeline. It is possible to see the intermediate steps, such as segmentation and tracking [6].

2.11 Statistical comparison of groups

To evaluate differences between glucose conditions, statistical hypothesis testing is commonly used to compare whether observed differences in measured features are likely to arise from random variation or reflect true underlying differences. In this study, Welch's t-test was used, which does not assume equal variance between groups and is therefore suitable for biological data with potentially unequal variability[19].

The test is applied under the null hypothesis that the means of two groups are equal, and a p-value is computed to assess the probability of observing the measured difference under this assumption[19].

Chapter 3

Method

This chapter describes the experimental and computational methods used to investigate mitochondrial dynamics under differing glucose conditions. Section 3.1 outlines the cell culture procedures, including preparation of the MDCK II cell line, culture conditions, passaging and sample preparation prior to imaging. Section 3.2 describes the glucose treatment conditions and preparation of experimental media.

Section 3.3 presents the microscopy setup and live-cell imaging parameters used for time lapse acquisition of mitochondrial fluorescence signals. Section 3.4 describes the image processing workflow and mitochondrial tracking performed using the Nellie framework [6]. Section 3.5 explains the MSD analysis, trajectory filtering procedures and extraction of quantitative motion descriptors. Finally, Section 3.6 introduces the AI-based image analysis pipeline used for comparative analysis against the Nellie-based workflow.

3.1 Cell Culturing

3.1.1 Cell Line and Culture Medium

MDCK II cells transduced with mitochondria-targeted green fluorescent protein (mito-GFP) were used throughout the project. The cells were cultured in a T-25 flask and kept in an incubator at 37.00 °C and 5.00 % CO₂.

A complete culture medium was prepared using Eagle's minimum essential medium (EMEM) as a base, supplemented with 1.00 % penicillin-streptomycin, 1.00 % L-glutamine and 5.00 % fetal bovine serum (FBS). To prepare 500 mL of complete medium, 35 mL of minimum essential medium

(MEM) was removed from the original bottle and then replaced with 5mL penicillin-streptomycin, 5 mL L-glutamine and 25 mL FBS.

3.1.2 Cell Thawing and Passaging

Frozen cells were thawed in a 37.00 °C water bath, then transferred to a 15 mL tube with warmed complete medium. The suspension was then centrifuged, whereafter the supernatant was discarded. The cell pellet was resuspended in fresh complete medium and transferred to a T-25 culture flask containing already warmed complete medium. The cells were then maintained at 37.00 °C in a humidified incubator with 5.00 % CO₂ and 90.00 % relative humidity (RH).

Cell splitting was performed twice a week at approximately 70.00 % confluency. The medium was removed from the T-25 flask and the cells were washed twice with phosphate-buffered saline (PBS). Trypsin was added to detach the cells from the flask, and the flask was then incubated until cells were detached, approximately 12 minutes. Cells were then resuspended in complete medium and transferred to a new T-25 flask containing pre-warmed complete medium. Cells were split at a 1:10 ratio. The cells were then returned to the incubator. The full cell culturing protocol can be found in Appendix A.

3.1.3 Imaging Preparation

When preparing cells for microscopy, the cells were seeded into 35 mm MatTek glass-bottom dishes. Each dish contained 2 mL of warmed complete medium. To this, 50 µL of the cell suspension was added. Cells were then allowed to grow for three days to approximately 50.00 % confluency before imaging took place.

3.2 Glucose Treatment

Cells were cultured under three glucose conditions: low glucose, baseline (normal culture medium), and high glucose, to investigate the effects of glucose availability on mitochondrial dynamics. The corresponding glucose concentrations are summarised in Table 3.1.

The baseline medium used was normal culture medium. The high glucose medium and low glucose medium needed to be mixed. The composition of the culture medium was used to calculate the osmolarity of the different glucose conditions. Because glucose contributes to osmolarity in the culture

Table 3.1: Glucose concentrations used for the different culture conditions.

Condition	Glucose concentration (mmol/L)
Baseline (Physiological)	5.5
High glucose	20
Low glucose	0

medium, the sugar alcohol mannitol was added to the glucose free medium to maintain the osmotic balance, without being metabolized by the cells. Medium compositions were calculated to achieve osmolarities comparable to a standard culture medium (approximately 280 - 310 mOsm/L). This was done to ensure that any effects on mitochondrial dynamics were caused by differences in glucose availability, not osmotic stress.

The major contributors to osmolarity were inorganic salts, while amino acids and vitamins contributed smaller amounts. The calculated osmolarities are summarised in Tables 3.2 and 3.3. The full composition of the glucose medium can be found in Appendix B.

Table 3.2: Composition of inorganic salts used in the culture medium and their calculated osmolarity contributions.

Ingredient	Amount (mg/L)	Molar weight (g/mol)	Van't Hoff factor	Osmolarity (mOsm/L)
CaCl ₂	265	146.0	3	5.44
MgSO ₄	97.67	120.37	2	1.62
KCl	400	74.55	2	10.73
NaHCO ₃	2200	84.00	2	52.37
NaCl	6350	58.44	2	217.32
NaH ₂ PO ₄	122	119.98	2	2.03
Total osmolarity				289.51

Table 3.3: Additional organic components present in the culture medium.

Component group	Total osmolarity contribution (mOsm/L)
Amino acids	4.85
Vitamins	0.06

To prepare the different glucose conditions, glucose and mannitol concentrations were calculated based on their molar masses. The molar mass of glucose is $180.16 \text{ g mol}^{-1}$, corresponding to:

$$20 \text{ mmol L}^{-1} \times 180.156 \text{ mg mmol}^{-1} = 3603.12 \text{ mg L}^{-1} \quad (3.1)$$

Mannitol was used for osmotic balancing in the low glucose condition. The molar mass of mannitol is $182.17 \text{ g mol}^{-1}$, corresponding to:

$$20 \text{ mmol L}^{-1} \times 182.17 \text{ mg mmol}^{-1} = 3643.4 \text{ mg L}^{-1} \quad (3.2)$$

The final osmolarity of the glucose- and mannitol-adjusted media was approximately 314.41 mOsm/L , which closely matched the osmolarity of the standard culture medium.

Prior to imaging, the cells were washed twice with PBS to remove residual culture medium and glucose. The cells were then incubated in their respective treatment media for one hour before microscopy imaging. This incubation period allowed the cells to adapt to the altered glucose conditions prior to time lapse acquisition.

3.3 Microscopy

Microscopy was performed using a Zeiss Axio Observer Z1 widefield fluorescence microscope equipped with a Colibri 7 LED illumination system, a 63x oil immersion objective, and an objective heater to maintain physiological temperature during imaging.

The microscope was allowed to warm up for at least one hour prior to imaging acquisition, to ensure stable imaging conditions. Immersion oil was applied to the objective, and glass-bottomed dishes containing cells were placed on the microscope stage, in a $5.00\% \text{ CO}_2$ chamber. Cells were allowed to equilibrate on the microscope for one hour prior to imaging to minimize drifting.

Mitochondria were visualized using mito-GFP fluorescence with excitation in the AF488 channel. Time-lapse image acquisition was performed using the ZEN software [20]. The imaging parameters are summarised in Table 3.4.

Images were acquired at a rate of one frame per second for a total of 600 cycles, corresponding to a total imaging duration of 10 minutes. Focus was adjusted to ensure image quality prior to acquisition. When the time lapse was completed, it was saved in CZI file format.

Table 3.4: Microscopy acquisition settings used for time-lapse imaging of mitochondria.

Parameter	Setting
Fluorescence label	mito-GFP (AF488 channel)
Software	ZEN software [20]
Acquisition mode	Gated acquisition
Binning	1 × 1
LED power	5–15%
Exposure time	200 ms
Grey filter level	5/6
Region of interest (ROI)	1024 × 1024 pixels
Frame rate	1 frame/s
Total frames	600
Total duration	10 min
File format	CZI

3.4 Image Processing and Mitochondrial Tracking

After image acquisition, microscopy data were processed to extract mitochondrial trajectories for quantitative analysis. Time lapses acquired in CZI format were converted to TIFF format using Fiji [21], as the CZI format is not supported by the analysis software. Images were cropped to regions containing a single cell to reduce computational load and focus the analysis on a single cell, while maintaining temporal resolution.

Nellie, the Python-based framework, was used to perform mitochondrial segmentation and tracking. Image metadata and acquisition parameters, including spatial and temporal resolution, were verified prior to analysis. Nellie identified mitochondrial structures and reconstructed their morphology and movement over time by linking segmented features across sequential frames.

The analysis pipeline generated several output csv files containing quantitative descriptors of mitochondrial structures and trajectories. The file `features_organelles` was used for the analysis, as it contained information on mitochondrial positions and their temporal evolution. The exported data was then further processed in Excel to ensure correct formatting and separation of variables before computational analysis was performed.

3.5 MSD and Trajectory Analysis

A custom Python pipeline was created to analyse single-particle trajectories and calculate MSD. The script was based on NumPy, pandas and scikit-learn. Eight biological replicates from each glucose condition (20 mM glucose, 0 mM glucose and 5.5 mM glucose) were utilised. Each biological replicate corresponded to an independently acquired time lapse recording from a separate imaging field. The csv files produced by the Nellie pipeline were imported and trajectories for each particle were created based on their x and y positions at each time point. The trajectories were then averaged per time point to reduce segmentation noise.

For each trajectory, the MSD was calculated as shown in Equation (3.3).

$$\text{MSD}(\tau) = \left\langle (x(t + \tau) - x(t))^2 + (y(t + \tau) - y(t))^2 \right\rangle \quad (3.3)$$

τ represented the lag time in frames, each frame corresponding to one second. For each particle trajectory, the TAMSD was computed by averaging squared displacements over all valid time origins. MSD was calculated for all lag times from $\tau = 1$ up to $\tau = N - 1$, where N was the trajectory length. Filtering was used to exclude all trajectories with fewer than 30 time points to avoid unstable fits and increase the robustness of the estimation. A qualitative validation of the MSD analysis is provided in Appendix C.

For each particle, the MSD curve was analysed on a log-log scale to quantify their movement. The power law from Equation (2.2) was assumed. α was estimated for each particle by fitting a linear regression model to:

$$\log(\text{MSD}) = \alpha \log(\tau) + C \quad (3.4)$$

The fit was performed over a restricted fitting range to reduce bias from noisy long-lag estimates and short time noise effects. The following criteria were used for inclusion in the fitting:

- $\tau > 1$
- $\tau < 85\text{th percentile of available lag times}$
- $\text{MSD} > 0$
- At least 5 valid data points per fit
- $0 \leq \alpha \leq 2$

Based on Equation (3.5), each particle was then classified.

$$\begin{aligned}
 \text{Confined motion: } & \alpha < 0.9 \\
 \text{Brownian motion: } & 0.9 \leq \alpha < 1.1 \\
 \text{Active motion: } & \alpha \geq 1.1
 \end{aligned} \tag{3.5}$$

The proportion of each motion class was computed per glucose condition.

For each single particle trajectory, additional features including step displacement, velocity and confinement ratio were calculated.

Step displacement was calculated as shown in Equation (3.6). Velocity was calculated as shown in Equation (3.7), and the confinement ratio was calculated as shown in Equation (3.8).

$$\Delta r = \sqrt{(\Delta x)^2 + (\Delta y)^2} \tag{3.6}$$

$$v = \frac{\Delta r}{\Delta t} \tag{3.7}$$

$$\text{Confinement ratio} = \frac{\text{net displacement}}{\text{total path length}} \tag{3.8}$$

All three features were averaged per time lapse and then per glucose condition.

To compare the different glucose conditions, all MSD curves from each condition were averaged. As the trajectories had differing lengths, the MSD values were aligned by their lag time and then averaged using aggregation while ignoring missing values (NaN values) over all particles.

Differences between the glucose conditions were assessed using Welch's t-test on alpha values (per trajectory mean), mean velocity and step displacement. The significance was assessed using two-sided tests. Statistical significance was defined as $p < 0.05$.

3.6 AI-based Pipeline

To compare the results obtained from Nellie and the custom Python pipeline, a separate AI-based image segmentation pipeline was created using the Claude large language model [22]. The model was prompted to generate a Python-based workflow inspired by established bioimage analysis frameworks, including Cellpose-style segmentation approaches [23], and iteratively refine the implementation through structured feedback.

The resulting pipeline processed the entire ROI for each time lapse recording, in contrast to the Nellie-based pipeline which analyzed a single selected cell per time lapse to reduce computational load. In total, the AI pipeline analyzed 15 high glucose time lapses and 13 low glucose time lapses, but did not include time lapses with the baseline glucose condition. The Nellie-based pipeline instead used 24 time lapses in total, and eight time lapses per condition: baseline, high glucose and low glucose.

Image analysis consisted of automated segmentation of mitochondrial structures followed by object tracking across frames. From the resulting trajectories, quantitative motility descriptors were extracted. For consistency with the Nellie-based pipeline, only the following features were used for direct comparison: MSD, anomalous diffusion exponent (α), step displacement, velocity, and confinement ratio.

Although the AI pipeline also generated additional morphological and network-related descriptors (e.g., shape and connectivity metrics), these were not included in the present analysis, as they were not computed in the corresponding Nellie-based workflow.

For MSD analysis, trajectories were used to compute:

$$\text{MSD}(\tau) = \langle |\mathbf{r}(t + \tau) - \mathbf{r}(t)|^2 \rangle \quad (3.9)$$

The anomalous diffusion exponent α was obtained by linear regression on the log-log transformed MSD:

$$\log(\text{MSD}) = \alpha \log(\tau) + C \quad (3.10)$$

All feature extraction and statistical processing were performed in Python, and the AI-generated pipeline outputs were used solely as a comparative dataset against the Nellie-based analysis.

The AI system also generated a structured analytical report summarising the pipeline design, intermediate outputs, and results. This report was used for documentation and verification purposes, but only quantitative outputs (MSD-derived metrics and motility descriptors) were used for analysis.

Chapter 4

Results

This chapter presents the quantitative results obtained from the analysis of mitochondrial trajectories under differing glucose conditions. Section 4.1 provides an overview of the analysed dataset and extracted motion descriptors. Section 4.2 presents the MSD analysis used to characterize mitochondrial movement across glucose conditions. Section 4.3 describes the classification of mitochondrial motion based on anomalous diffusion behaviour and estimated α -values.

Section 4.4 presents additional trajectory-derived motility descriptors, including velocity, confinement ratio and step displacement. Section 4.5 summarises the statistical comparisons performed between experimental conditions. Finally, Section 4.6 compares the results obtained using the Nellie-based analysis pipeline with those generated using the independent Claude AI-based image analysis pipeline.

4.1 Overview of Dataset

A representative example of microscopy images from the baseline glucose condition is shown in Figure 4.1. The images illustrate the appearance of mitochondria in living MDCK II cells and provide an overview of the image processing workflow. Figure 4.1a and Figure 4.1b show the original ROI and the corresponding cropped image used as input into Nellie. Figure 4.1c- 4.1f show the successive steps performed by the Nellie pipeline.

Mitochondria appeared as interconnected tubular structures with varying intensity and morphology. In several regions, mitochondrial structure overlapped or formed dense local networks, making individual organelles difficult to distinguish manually. Variability in fluorescence intensity and

structural complexity further complicates segmentation and tracking.

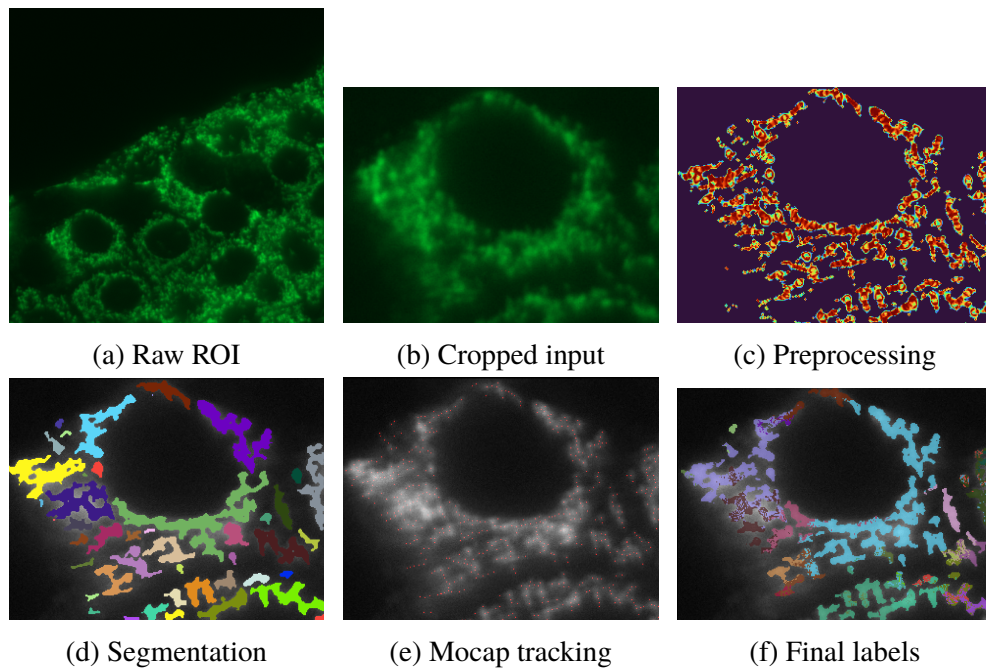


Figure 4.1: Overview of the mitochondrial image analysis workflow using the Nellie framework. a) Raw fluorescence microscopy image of MDCK II cells. b) Cropped region used for analysis. c) Preprocessed image after enhancement. d) Segmentation of mitochondrial structures. e) Mocap-based motion tracking. f) Reassigned organelle labels used for trajectory extraction.

Table 4.1 summarises the dataset used for subsequent MSD analysis. A total of 213, 224, and 284 mitochondrial trajectories were extracted for high glucose, low glucose, and baseline conditions respectively, across eight independent time lapse recordings per condition. For each trajectory, multiple motion descriptors were computed, including the MSD, anomalous diffusion exponent (α), velocity, confinement ratio and step displacement. These metrics form the basis for the quantitative comparisons between glucose conditions.

Table 4.1: Overview of analysed mitochondrial trajectory dataset.

Condition	Number of trajectories	Number of time-lapses
High glucose	213	8
Low glucose	224	8
Baseline	284	8

4.2 Mitochondrial Movement Assessed by MSD Analysis

To quantify mitochondrial motility across different glucose conditions, MSD analysis was performed on all extracted mitochondrial trajectories. MSD increased with increasing lag time for all conditions, indicating continued mitochondrial displacement over time. The overall shapes of the MSD curves were similar across the different glucose conditions, suggesting that the general characteristics of mitochondrial motion remained. Differences between glucose conditions were modest, although slightly higher MSD values were shown for the high glucose condition, in comparison to the low glucose and baseline conditions.

The ensemble-averaged MSD curves for each condition are shown in Figure 4.2. Representative MSD values at lag times $\tau = 1$ and $\tau = 5$ are summarised in Table 4.2.

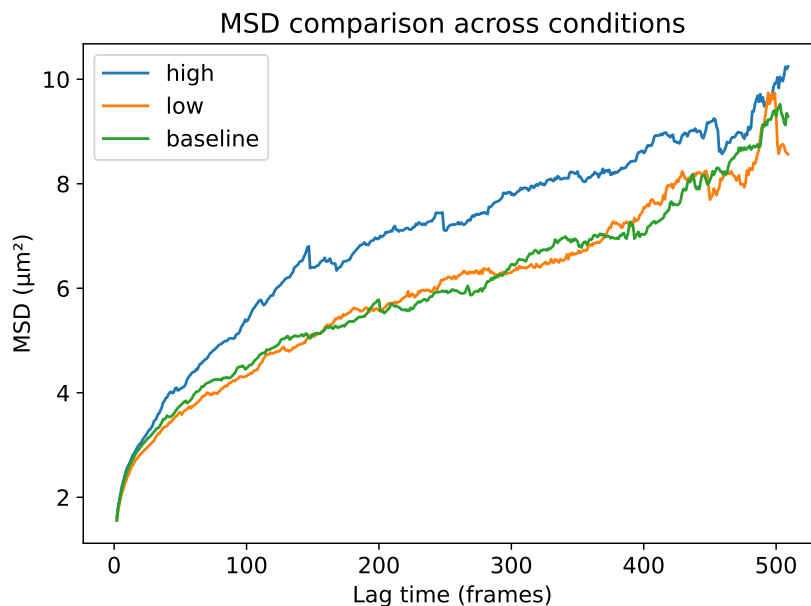


Figure 4.2: MSD curves of mitochondrial trajectories under differing glucose conditions. MSD increased with lag time in all conditions, with high glucose showing slightly elevated displacement values compared to low glucose and baseline conditions.

Table 4.2: Mean squared displacement (MSD) values evaluated at lag times $\tau = 1$ and $\tau = 5$ for each glucose condition.

Condition	MSD $\tau = 1$	MSD $\tau = 5$
High glucose	1.62	2.23
Low glucose	1.55	2.10
Baseline	1.56	2.18

4.3 Motion Classification

To characterise mitochondrial motion behaviour, anomalous diffusion exponents (α) were calculated from MSD slopes for individual trajectories. The mean α values vary slightly across conditions, with the highest mean value observed in the high glucose condition. α distribution across glucose conditions can be seen in Figure 4.3.

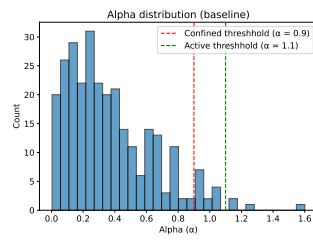
The distributions of calculated α -values were broad for all conditions, with most trajectories located within the subdiffusive regime ($\alpha < 1$). A relatively small proportion of trajectories showed values consistent with Brownian or active motion. Histograms of the estimated α -values are presented in Figure 4.3.

The mean α values were 0.47 ± 0.36 for the high glucose condition, 0.42 ± 0.32 for the low glucose condition and 0.37 ± 0.27 for the baseline condition. Across all conditions, confined motion was dominant. 84.50% of trajectories were classified as confined in the high glucose condition, while the same classification was 90.20% in the low glucose condition and 94.00% in the baseline condition. The full classification proportions can be seen in Table 4.3.

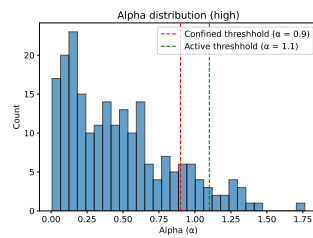
Although variability between individual trajectories was observed, the fitted relationships remained approximately linear on the logarithmic scale for all conditions, supporting the use of a power-law model for estimation of the anomalous diffusion exponent α (Figure 4.4).

Table 4.3: Summary of anomalous diffusion exponent (α) values and motion classification percentages across glucose conditions.

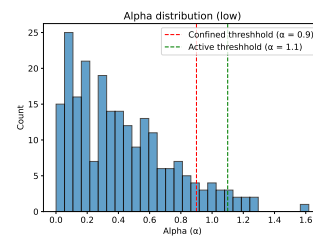
Condition	Mean $\alpha \pm$ SD	Confined (%)	Brownian (%)	Active (%)
High glucose	0.47 ± 0.36	84.5	8.5	7.0
Low glucose	0.42 ± 0.32	90.2	5.8	4.0
Baseline	0.37 ± 0.27	94.0	4.6	1.4



(a) Baseline

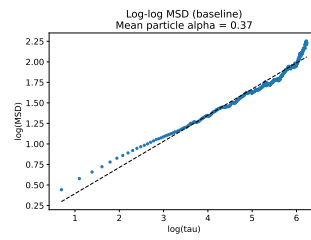


(b) High glucose

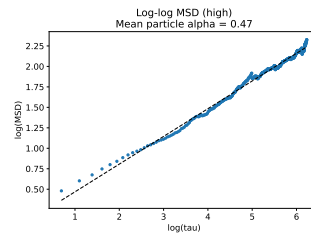


(c) Low glucose

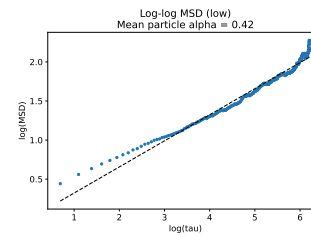
Figure 4.3: Distribution of anomalous diffusion exponents (α) across glucose conditions.



(a) Baseline glucose



(b) High glucose



(c) Low glucose

Figure 4.4: Log-log plots of mean squared displacement (MSD) as a function of lag time for mitochondrial trajectories under different glucose conditions. The slope of the fitted relationship corresponds to the anomalous diffusion exponent α , which describes the scaling behaviour of mitochondrial motion.

4.4 Velocity, Confinement and Displacement

Trajectory-derived mitochondrial motion descriptors were analysed to complement the MSD-based analysis and provide additional information regarding mitochondrial movement behaviour. These descriptors quantify different aspects of mitochondrial motion, including instantaneous displacement between frames, overall movement speed and the degree of confinement during trajectory progression.

Measurements obtained from individual biological replicates showed variability within each glucose condition, although overall trends remained similar between conditions. The highest replicate-level values for both step displacement and velocity were observed in isolated recordings within the low and high glucose conditions, while confinement ratios remained relatively low across all datasets. Mean step displacement and velocity were generally similar across all three glucose conditions, although slightly elevated values could be observed in the high glucose condition, compared to the low glucose and baseline conditions.

The mean step displacement values were 0.55 ± 0.63 for the high glucose condition, 0.50 ± 0.65 for the low glucose condition and 0.53 ± 0.60 for the baseline condition. Mean velocity values were 0.50 ± 0.63 for high glucose, 0.45 ± 0.64 for low glucose and 0.46 ± 0.60 for baseline conditions. Mean confinement ratio was 0.05 ± 0.07 for high glucose, 0.04 ± 0.06 for low glucose and 0.03 ± 0.05 for the baseline condition. Table 4.4 shows the velocity, step displacement and confinement ratio per biological replicate while Table 4.5 shows a summary across glucose conditions.

Overall, the trajectory-derived motion descriptors showed relatively similar distributions across all glucose conditions. Slightly elevated step displacement and velocity values were observed for the high glucose condition, while confinement ratio values remained low across all analysed datasets.

Table 4.4: Mitochondrial mean step displacement, velocity and confinement ratio for each biological replicate.

Condition	Rep.	Step	Velocity	Confinement
High	1	0.56	0.51	0.05
High	2	0.50	0.46	0.05
High	3	0.39	0.34	0.08
High	4	0.60	0.54	0.07
High	5	0.92	0.82	0.01
High	6	0.62	0.57	0.05
High	7	0.62	0.55	0.03
High	8	0.45	0.41	0.04
Low	9	0.41	0.38	0.05
Low	10	0.42	0.38	0.03
Low	11	0.26	0.23	0.04
Low	12	1.17	1.10	0.04
Low	13	0.57	0.52	0.03
Low	14	0.49	0.43	0.04
Low	15	0.44	0.40	0.05
Low	16	0.70	0.58	0.08
Baseline	17	0.62	0.55	0.05
Baseline	18	0.51	0.43	0.04
Baseline	19	0.50	0.41	0.03
Baseline	20	0.51	0.46	0.03
Baseline	21	0.48	0.42	0.02
Baseline	22	0.73	0.65	0.04
Baseline	23	0.47	0.41	0.03
Baseline	24	0.52	0.46	0.04

Table 4.5: Summary of mitochondrial motion descriptors across glucose conditions.

Condition	Step displacement (mean \pm SD)	Velocity (mean \pm SD)	Confinement ratio (mean \pm SD)
High glucose	0.55 \pm 0.63	0.50 \pm 0.63	0.05 \pm 0.07
Low glucose	0.50 \pm 0.65	0.45 \pm 0.64	0.04 \pm 0.06
Baseline	0.53 \pm 0.60	0.46 \pm 0.60	0.03 \pm 0.05

4.5 Statistical Comparison

Pairwise statistical comparisons were performed between all glucose conditions for the extracted mitochondrial motion parameters. Comparisons included the anomalous diffusion exponent (α), velocity, confinement ratio and step displacement. The resulting p-values are presented in Table 4.6.

Table 4.6: Pairwise p-values between glucose conditions for MSD-derived metrics.

Metric	High vs Low	High vs Baseline	Low vs Baseline
α -value	0.42	0.22	0.73
Velocity	0.38	0.50	0.77
Confinement ratio	0.52	0.015	0.06
Step displacement	0.35	0.66	0.56

Most comparisons produced p-values above the predefined significance threshold of $p < 0.05$, indicating that the measured differences between glucose conditions were generally modest relative to the observed variability within the datasets; however, confinement ratio measurements differed significantly between the high glucose and baseline conditions, while comparisons involving low glucose conditions did not show statistical significance.

4.6 Nellie and Claude AI Pipeline Comparison

To evaluate the consistency of the mitochondrial motion analysis, the results obtained using the Nellie-based pipeline were compared with outputs

generated from a Claude AI-based pipeline. The pipelines were both applied to fluorescence microscopy time lapses acquired under high and low glucose conditions, although the Claude AI pipeline included a larger number of datasets than the analysis based on Nellie.

The comparison between pipelines focused on metrics that were independently extracted by both analysis approaches. These included MSD, anomalous diffusion exponent (α), velocity, confinement ratio and step displacement. Although the computational strategies differed substantially between pipelines, both approaches aimed to quantify mitochondrial motion behaviour from the fluorescence microscopy recordings.

The Nellie-based pipeline and the Claude AI pipeline identified similar overarching trends in mitochondrial displacement, but with differences in absolute values. Both approaches showed increasing MSD values with increasing lag time and modest differences between high and low glucose conditions.

The Claude AI pipeline showed that the ensemble MSD at $\tau = 5$ was 1.50 ± 1.26 for high glucose and 1.34 ± 1.22 for low glucose. Values obtained using the Nellie pipeline were 2.23 and 2.10, respectively. For the Nellie pipeline, standard deviations for MSD were not included in the comparison. MSD values are reported as condition-level summary statistics rather than full trajectory-wise distributions. Consequently, variability measures such as standard deviation were not calculated for MSD at fixed lag times.

Both pipelines found mitochondrial motion to be predominantly confined across both high and low glucose conditions. The Claude AI pipeline found mean α -values of 0.61 ± 0.05 for high glucose and 0.57 ± 0.07 for low glucose, while the Nellie pipeline yielded lower mean α -values of 0.47 ± 0.36 and 0.42 ± 0.32 , respectively.

Overall, both pipelines showed slightly elevated α -values under high glucose conditions compared to low glucose conditions, despite differences in absolute magnitude. Direct quantitative comparisons between the pipelines are summarised in Table 4.7. While absolute values differed between pipelines, the overall directional trends between high and low glucose conditions remained similar.

Variability estimates also differed between pipelines. In particular, the Claude AI pipeline generally produced narrower standard deviations for several motion descriptors compared to the Nellie-based analysis. Despite these quantitative differences, both approaches consistently classified mitochondrial motion as predominantly confined.

None of the pipelines identified statistically significant differences between

Table 4.7: Comparison of mitochondrial motion descriptors obtained using the Nellie and Claude AI analysis pipelines.

Metric	Nellie High	Nellie Low	Claude High	Claude Low
Mean α	0.47 ± 0.36	0.42 ± 0.32	0.61 ± 0.05	0.57 ± 0.07
MSD $\tau = 5$	2.23	2.10	1.50 ± 1.26	1.34 ± 1.22
Step displacement	0.55 ± 0.63	0.50 ± 0.65	0.35 ± 0.18	0.31 ± 0.17
Velocity	0.50 ± 0.63	0.45 ± 0.64	0.37 ± 0.19	0.35 ± 0.18
Confinement ratio	0.05 ± 0.07	0.04 ± 0.06	0.42 ± 0.05	0.40 ± 0.02

high and low glucose conditions for the motion descriptors analysed. For the Claude AI pipeline, p-values for α , MSD, velocity, confinement ratio and step displacement exceeded 0.05 for all pairwise comparisons. This is consistent with the predominantly non-significant findings observed using Nellie.

Overall, both pipelines produced comparable trends in mitochondrial dynamics across high and low glucose conditions, including predominantly confined motion and slight increases in motility under high glucose conditions. Quantitative parameter values, however, were observed to differ between pipelines.

Chapter 5

Discussion

This chapter discusses the biological interpretation and methodological implications of the results obtained in this study. Section 5.1 examines the predominantly confined nature of mitochondrial motion observed across all glucose conditions, while Section 5.2 discusses the potential effects of altered glucose availability on mitochondrial dynamics and cellular metabolism.

Section 5.3 addresses limitations of the study, including imaging-related challenges, biological variability and computational constraints associated with trajectory extraction and quantitative analysis. Section 5.4 compares the performance and outputs of the Nellie-based and Claude AI-based computational pipelines, with emphasis on differences in extracted motion descriptors and analysis strategies. Finally, Section 5.5 evaluates the strengths and limitations of the Nellie framework in the context of mitochondrial tracking and live-cell microscopy analysis.

5.1 Predominantly Confined Mitochondrial Motion

Mitochondrial motion was predominantly classified as confined across all three glucose conditions and both analysis pipelines. This was reflected by mean anomalous diffusion exponents (α) below 1. Only a relatively small fraction of trajectories exhibited behaviour consistent with Brownian or actively directed motion.

Confined motion is biologically plausible in the intracellular environment, as organelle movement occurs within a spatially crowded cytoplasm. Mitochondria are physically constrained by surrounding cellular structures,

including the cytoskeleton, other organelles and the cell itself. The predominance of confined trajectories observed is therefore consistent with the expectation that mitochondrial movement inside living cells is restricted.

Additionally, mitochondrial morphology may further complicate trajectory behaviour. Mitochondria form dynamic networks which undergo both fusion and fission, which make them more difficult to track compared to more stable particles. As a result, measured trajectories may reflect a combination of genuine mitochondrial transport, structural rearrangements, as well as limitations associated with computational tracking approaches.

MSD provides a useful first approximation of intracellular transport behaviour, but might not fully capture the complexity of mitochondrial dynamics within living cells. Intracellular motion analysis is strongly influenced by both biological complexity and experimental conditions [16], [17]. The consistent observation of predominantly confined motion across both analysis pipelines as well as independent of glucose condition does, however, suggest that this represents a robust feature of the analysed mitochondrial motion.

5.2 Effects of Glucose

Although mitochondrial motion remained predominantly confined under all analysed glucose conditions, several motility descriptors showed modest increases under high glucose conditions compared to low glucose and baseline conditions. A higher glucose condition was associated with slightly elevated MSD values, α -values, velocity measurements and step displacement values in both the Nellie-based and Claude AI-based analysis pipelines. These observations may suggest a tendency toward increased mitochondrial motility when there is a higher glucose availability within a cell.

Availability of glucose plays a central role in cellular energy metabolism and may therefore influence mitochondrial behaviour and intracellular transport dynamics. Increased glucose levels could potentially alter availability of ATP, cytoskeletal activity, or metabolic demand, which in turn may affect mitochondrial movement within the cell. The observed differences between glucose conditions were, however, generally modest, and most pairwise comparisons did not reach statistical significance. Importantly, lack of statistical significance does not necessarily imply absence of biological effects, particularly in studies with limited sample size and substantial biological variability.

The observed trend toward increased motility under high glucose

conditions is consistent with the initial hypothesis proposed in this thesis. Because mitochondrial transport is an active process dependent on ATP-driven motor proteins, increased glucose availability could potentially support mitochondrial transport by increasing cellular energy availability. Higher glucose conditions may therefore contribute to slightly elevated mitochondrial displacement and velocity. Additionally, glucose availability could influence mitochondrial morphology and network organisation, which further could affect motility patterns. Because the observed effects were relatively small, the relationship between glucose concentration and mitochondrial motility is likely influenced by several overlapping biological mechanisms.

The limited statistical separation between conditions may have occurred due to several factors. Mitochondrial movement within living cells is inherently diverse, with substantial variability from trajectory to trajectory, observed even within the same experimental condition. Additionally, the relatively small number of analysed time lapse recordings may have reduced statistical power and limited the ability to detect subtle biological differences.

Another factor that may have affected the results is the fact that motion descriptors were averaged over entire time lapses. This could have obscured time-dependent changes in mitochondrial dynamics. During manual inspection of several time lapses, mitochondrial movement appeared to vary throughout the imaging period, with some cells exhibiting more active movement during the early stages of recording, followed by reduced motility later in the time lapse. Such temporal variations may not be fully captured by ensemble MSD averages, or by other motion descriptors summarized on glucose condition-level.

Overall, the results suggest that glucose availability may influence aspects of mitochondrial motility, although the effects observed in this project were subtle and influenced by biological variability and methodological limitations.

5.3 Methodological Limitations

Interpretation of mitochondrial motion in living cells is influenced by multiple experimental and computational factors, associated with fluorescence microscopy imaging and trajectory analysis. In this project, there are several methodological limitations which may have affected the accuracy, reproducibility and interpretation of extracted mitochondrial motion parameters, which will be discussed in the following sections.

5.3.1 Imaging Limitations

The measured mitochondrial dynamics may have been influenced by several experimental factors associated with fluorescence microscopy imaging. Accurate quantification of intracellular motion depends strongly on imaging stability, focus consistency and maintenance of physiological cellular conditions throughout time lapse acquisition.

Temperature control may have influenced mitochondrial motility measurements. Although an objective heater was used during imaging, it did not consistently maintain physiological temperature conditions (37.00 °C) comparable to those of the incubator environment. Even small temperature reductions can substantially decrease mitochondrial dynamics [10], suggesting that deviations from optimal temperature may have reduced observed mitochondrial motility.

Small positional drift may have occurred during imaging despite allowing samples to equilibrate on the microscope prior to imaging. While no major mechanical movement was observed, subtle drift or focus instability may still have contributed to variability in extracted trajectory measurements.

5.3.2 Biological Variability

Biological variability between experimental samples may have contributed to variability in measured mitochondrial motion parameters. Although imaging was primarily performed using cells below passage 22, differences in passage number may have influenced cellular morphology and mitochondrial behaviour. At higher passage numbers, some cells displayed altered morphology with a more elongated or fibroblast-like appearance, suggesting potential phenotypic variation within the cultured population.

Variability in cell confluency may also have affected mitochondrial dynamics. While imaging was performed at approximately 50.00% confluency, precise assessment of confluency was subjective and likely varied somewhat between experiments. Differences in cell density can influence cellular morphology, intracellular organisation and metabolic state, all of which might affect the behaviour of mitochondrial motion.

Additionally, only one cell was analysed per time lapse in order to reduce the computational load and maintain manageable processing times during the Nellie analysis. While this allowed trajectory extraction from individual cells, it could have limited the extent to which analysed trajectories represented the full variability of the cell population.

5.3.3 Computational Limitations

Other limitations are associated with the computational analysis workflow. Mitochondria represent highly dynamic and structurally complex organelles, which are capable of fusion, fission and network rearrangement. Therefore, mitochondrial trajectories may not behave as stable particle-like objects. This could potentially complicate automated trajectory extraction and motion classification.

The Nellie framework tracks segmented mitochondrial structures rather than discrete biologically isolated particles. As a result, measured trajectories may reflect changes in mitochondrial morphology or segmentation behaviour in addition to genuine intracellular transport. This may be particularly relevant during mitochondrial fusion and fission, where trajectory continuity becomes difficult to define computationally.

Some preprocessing decisions were also made during data analysis, which might affect the outcome. Time lapse recordings were cropped using rectangular ROI instead of freehanded cell outlines, as freehand cropping introduced segmentation artefacts during Nellie processing. Additionally, some extracted datasets contained duplicate trajectory entries that required additional cleaning during Python analysis.

The MSD-based analysis of trajectories itself contains important assumptions and limitations. Although MSD provides a useful first approximation of mitochondrial motility behaviour, extracted motion parameters are sensitive to uncertainty, trajectory length and fitting strategy [16].

5.4 Computational Pipeline Comparison

When comparing the Nellie and Claude AI analysis pipelines, substantial qualitative agreements in the overall interpretation of mitochondrial dynamics were revealed. Both approaches showed predominantly confined mitochondrial motion across all analysed glucose conditions, while also detecting modest increases in motion-related parameters under high glucose conditions. Neither pipeline produced particularly significant statistical comparisons between glucose conditions, suggesting that the overall biological conclusions were relatively consistent despite methodological differences between the analysis approaches.

The AI-generated pipeline was accompanied by an automatically produced analytical report, including sections resembling a traditional scientific structure (introduction, methods, results, and discussion). While this was

useful for debugging and iterative refinement of the computational workflow, the interpretative content of the report was not used for biological conclusions. Instead, all scientific interpretations in this study were based solely on quantitatively derived metrics and statistical analysis.

Although the qualitative trends were similar, there were notable quantitative differences observed in several of the extracted motion parameters. Differences were particularly apparent for confinement ratio, anomalous diffusion exponents (α) and absolute MSD magnitudes. The Claude AI pipeline produced significantly larger confinement ratio values as well as systematically higher α -values, compared to the values obtained using Nellie.

Several factors may explain these quantitative discrepancies. The two pipelines relied on different computational strategies for trajectory extraction, preprocessing and motion parameter calculation. Even small differences in segmentation behaviour, trajectory filtering, handling of short trajectories or fitting procedures may substantially influence measurements. This is especially relevant for mitochondria, whose structures are highly dynamic and continuously undergo morphological change.

A direct comparison between both approaches was made more difficult by differences in composition of the dataset used. The Claude AI pipeline included a larger number of time lapse recordings and excluded baseline glucose conditions, while the Nellie analysis used a smaller subset of time lapses, together with an additional baseline condition. There were also differences in ROI selection and preprocessing workflows which also may have contributed to variability between pipelines.

Altogether, the findings suggest that trajectory-derived mitochondrial motion parameters are sensitive to the computational analysis workflow used. The consistent identification of confined mitochondrial motion and modest glucose-associated motility differences across both pipelines suggests that the broader qualitative conclusions of the project are relatively robust despite variability in exact numerical outputs.

5.5 Evaluation of Nellie

This project suggests that Nellie is capable of extracting biologically meaningful information from fluorescence microscopy of mitochondrial motion. The pipeline successfully generated mitochondrial trajectories across three different glucose conditions and produced motion descriptors consistent with expected intracellular behaviour, including predominantly confined motion. Additionally, Nellie identified modest increases in mitochondrial

motility under high glucose conditions, trends that were qualitatively consistent with those observed using the independent Claude AI analysis workflow.

Several aspects of the results derived from the Nellie pipeline support the biological plausibility of the extracted motion parameters. The predominance of confined trajectories is consistent with the spatially restricted intracellular environment in which mitochondria move. The ability of Nellie to reproduce similar qualitative trends across experimental conditions therefore suggests that the pipeline captures meaningful features of mitochondrial dynamics.

This project also highlighted important limitations associated with applying Nellie to mitochondrial trajectory analysis. Quantitative outputs were sensitive to preprocessing decisions, trajectory filtering and ROI selection. Additionally, some extracted datasets contained duplicate trajectory entries that required additional cleaning prior to analysis, indicating that post-processing quality control remained necessary.

Mitochondria also present a specific challenge for automated tracking approaches due to their dynamic morphology, as they continuously undergo fusion, fission and structural rearrangements. This makes trajectory continuity difficult to define computationally. Measured trajectories may therefore reflect both intracellular transport as well as changes in mitochondrial morphology or segmentation behaviour.

Overall, the findings in this project suggest that Nellie represents a useful tool for exploratory analysis of mitochondrial dynamics in fluorescence microscopy data, particularly for identifying qualitative trends in intracellular motion behaviour. The observed sensitivity of quantitative outputs to computational analysis choices highlights the importance of careful preprocessing, trajectory validation and complementary analysis approaches when interpreting extracted mitochondrial motion parameters. Future methodological improvements and expanded datasets may further improve the reliability and interpretability of mitochondrial trajectory analysis using automated computational workflows.

Chapter 6

Conclusion

6.1 Conclusion

This thesis set out to investigate mitochondrial dynamics in live MDCK II cells under three different glucose conditions using fluorescence microscopy combined with computational trajectory analysis. Mitochondrial motion was analysed using the Nellie tracking framework together with MSD-based motion analysis. The resulting measurements were compared with those obtained using an independent Claude AI-based analysis pipeline.

Across all analysed glucose conditions: high glucose, low glucose and baseline, mitochondrial motion was predominantly classified by confined behaviour, consistent with the spatially restricted intracellular environment in which mitochondria move. While the high glucose conditions were generally associated with modest increases in mitochondrial motility descriptors, including MSD, velocity and anomalous diffusion exponent values, most differences between glucose conditions remained statistically non-significant. These findings suggest that glucose availability may influence mitochondrial dynamics, although the observed effects were subtle and could be influenced by biological variability and methodological limitations.

Comparison between the Nellie-based pipeline and the Claude AI-based pipeline demonstrated a broad qualitative agreement in the overall interpretation of mitochondrial behaviour, although there were quantitative differences in extracted motion parameters. Both approaches consistently identified confined mitochondrial motion as the dominant transport pattern and detected similar overall glucose-associated trends. Together, these findings suggest that Nellie is capable of capturing biologically meaningful aspects of mitochondrial dynamics, while also highlighting the sensitivity

of trajectory-derived measurements to computational analysis strategy and preprocessing methodology.

Overall, this thesis demonstrates both the potential and the limitations of computational mitochondrial trajectory analysis in fluorescence microscopy data. The findings highlight the importance of careful experimental design, trajectory validation, and critical interpretation when analysing intracellular motion in living cells.

6.2 Future Work

There are several methodological and analytical improvements which could strengthen future investigations of mitochondrial dynamics using fluorescence microscopy and computational trajectory analysis. Increasing the number of analysed time lapses and including multiple cells per recording would improve statistical power and better capture biological variability within the cell population. Improved environmental control during microscopy, particularly in regards to temperature stability, may also increase the reliability of extracted motion parameters.

Future studies could also investigate time-dependent changes in mitochondrial motility, rather than relying exclusively on ensemble-averaged motion descriptors. Analysis of temporal variation within individual recordings may provide additional insight into transient changes in mitochondrial dynamics that are not fully captured by condition-level averaging approaches.

Finally, comparison of multiple independent computational analysis pipelines may help establish more robust and reproducible approaches for mitochondrial trajectory analysis. Integration of advanced machine learning or deep learning-based tracking methods may further improve segmentation accuracy and interpretation of complex intracellular motion behaviour in future studies.

References

- [1] M. C. Cooper and R. E. Hausman, *The Cell: A Molecular Approach*, 6th ed. Sinauer Associates, 2013.
- [2] H. Hoitzing, I. G. Johnston, and N. S. Jones, “What is the function of mitochondrial networks? a theoretical assessment of hypotheses and proposal for future research,” *BioEssays*, vol. 37, no. 6, pp. 687–700, 2015. doi: 10.1002/bies.201400188
- [3] P. Mishra and D. C. Chan, “Metabolic regulation of mitochondrial dynamics,” *Journal of Cell Biology*, vol. 212, no. 4, pp. 379–387, 2016. doi: 10.1083/jcb.201511036
- [4] R. Chaudhry and M. A. Varacallo. (2023) Biochemistry, glycolysis. StatPearls [Internet]. Treasure Island (FL): StatPearls Publishing. [Online]. Available: <https://www.ncbi.nlm.nih.gov/books/NBK482303/>
- [5] B. C. Mulukutla, A. Yongky, T. Le, D. G. Mashek, and W. Hu, “Regulation of glucose metabolism – a perspective from cell bioprocessing,” *Trends in Biotechnology*, vol. 34, no. 8, pp. 638–651, 2016. doi: 10.1016/j.tibtech.2016.04.012
- [6] A. E. Y. T. Lefebvre, G. Sturm, T. Y. Lin, E. Stoops, M. Preciado López, B. Kaufmann-Malaga, and K. Hake, “Nellie: automated organelle segmentation, tracking and hierarchical feature extraction in 2d/3d live-cell microscopy,” *Nature Methods*, vol. 22, pp. 751–763, 2025. doi: 10.1038/s41592-025-02612-7
- [7] L. C. Tábara, J. L. Morris, and J. Prudent, “The complex dance of organelles during mitochondrial division,” *Trends in Cell Biology*, vol. 31, no. 4, pp. 241–253, 2021. doi: 10.1016/j.tcb.2020.12.005

- [8] J. N. Meyer, T. C. Leuthner, and A. L. Luz, “Mitochondrial fusion, fission, and mitochondrial toxicity,” *Toxicology*, vol. 391, pp. 42–53, 2017. doi: 10.1016/j.tox.2017.07.019
- [9] E. L. Barnhart, “Mechanics of mitochondrial motility in neurons,” *Current Opinion in Cell Biology*, vol. 38, pp. 90–99, 2016. doi: 10.1016/j.ceb.2016.02.022
- [10] K. J. De Vos and M. P. Sheetz, “Visualization and quantification of mitochondrial dynamics in living animal cells,” in *Methods in Cell Biology*. Academic Press, 2007, vol. 80, pp. 627–682.
- [11] R. J. Giedt, D. R. Pfeiffer, A. Matzavinos *et al.*, “Mitochondrial dynamics and motility inside living vascular endothelial cells: Role of bioenergetics,” *Annals of Biomedical Engineering*, vol. 40, no. 9, pp. 1903–1916, 2012. doi: 10.1007/s10439-012-0568-6
- [12] J. D. Dukes, P. Whitley, and A. D. Chalmers, “The mdck variety pack: choosing the right strain,” *BMC Cell Biology*, vol. 12, p. 43, 2011. doi: 10.1186/1471-2121-12-43
- [13] A. Lakkaraju and E. Rodriguez-Boulan, “Epithelial cells,” in *Encyclopedic Reference of Genomics and Proteomics in Molecular Medicine*. Springer, 2006, pp. 516–523.
- [14] M. J. Sanderson, I. Smith, I. Parker, and M. D. Bootman, “Fluorescence microscopy,” *Cold Spring Harbor Protocols*, vol. 2014, no. 10, pp. 1042–1065, 2014. doi: 10.1101/pdb.top071795
- [15] R. Rizzuto, M. Brini, P. Pizzo, M. Murgia, and T. Pozzan, “Chimeric green fluorescent protein as a tool for visualizing subcellular organelles in living cells,” *Current Biology*, vol. 5, no. 6, pp. 635–642, 1995. doi: 10.1016/S0960-9822(95)00128-X
- [16] N. Gal, D. Lechtman-Goldstein, and D. Weihs, “Particle tracking in living cells: a review of the mean square displacement method and beyond,” *Rheologica Acta*, vol. 52, pp. 425–443, 2013. doi: 10.1007/s00397-013-0694-6
- [17] C. Schirripa Spagnolo and S. Luin, “Trajectory analysis in single-particle tracking: From mean squared displacement to machine learning approaches,” *International Journal of Molecular Sciences*, vol. 25, no. 16, p. 8660, 2024. doi: 10.3390/ijms25168660

- [18] napari contributors, “napari: a multi-dimensional image viewer for python,” 2019. [Online]. Available: <https://doi.org/10.5281/zenodo.3555620>
- [19] H. Motulsky, *Intuitive Biostatistics*, 4th ed. Oxford University Press, 2017.
- [20] Carl Zeiss Microscopy GmbH, “ZEISS ZEN Microscopy Software,” Carl Zeiss Microscopy GmbH, Jena, Germany, 2026, rRID:SCR_013672. [Online]. Available: <https://www.zeiss.com/microscopy/en/products/software/zeiss-zen.html>
- [21] J. Schindelin, I. Arganda-Carreras, E. Frise, V. Kaynig, M. Longair, T. Pietzsch, S. Preibisch, C. Rueden, S. Saalfeld, B. Schmid *et al.*, “Fiji: an open-source platform for biological-image analysis,” *Nature Methods*, vol. 9, no. 7, pp. 676–682, 2012. doi: 10.1038/nmeth.2019. [Online]. Available: <https://doi.org/10.1038/nmeth.2019>
- [22] Anthropic, “Claude,” <https://claude.ai>, 2025, large language model accessed for AI-assisted Python pipeline development.
- [23] C. Stringer, T. Wang, M. Michaelos, and M. Pachitariu, “Cellpose: a generalist algorithm for cellular segmentation,” *Nature Methods*, vol. 18, no. 2, pp. 100–106, 2021. doi: 10.1038/s41592-020-01018-x. [Online]. Available: <https://doi.org/10.1038/s41592-020-01018-x>

Appendix A

Cell Culture

The following protocol describes the routine maintenance, subculturing, and preparation of MDCK II cells used in this thesis. Cells were maintained at 37°C in a humidified incubator with 5% CO₂. Cells were passaged in T-25 flasks and seeded into 35 mm glass-bottom MatTek dishes for live-cell imaging experiments.

A.1 Materials

- MDCK II cells cultured in T-25 flasks
- Culture medium (EMEM supplemented with (5%) FBS, (1%) L-glutamine, and (1%) Penicillin-Streptomycin)
- Phosphate Buffered Saline (PBS)
- Trypsin-EDTA (0.25%)
- 5 mL serological pipettes
- Eppendorf pipettes and tips
- Waste bottle for liquid waste
- 35 mm glass-bottom MatTek dishes
- CO₂ incubator (37°C, 5% CO₂)
- Light microscope

A.2 Routine Subculturing

Cells were subcultured approximately twice per week using a 1:10 split ratio when reaching 70% confluency, assessed by light microscopy.

1. Culture medium, PBS, and trypsin-EDTA were prewarmed to 37°C.
2. Using a 5 mL pipette, the culture medium was removed from the T-25 flask containing cells. The culture medium was discarded in the waste bottle.
3. Cells were washed twice with 5 mL PBS to remove residual medium. The PBS was then discarded in the waste bottle.
4. 1 mL of trypsin-EDTA was added to the flask.
5. The flask was incubated at 37°C for approximately 12 minutes until cells detached, with periodic microscopic observation.
6. Cells were gently resuspended to obtain a homogeneous suspension.
7. A 1:10 fraction of the cell suspension was transferred to a new T-25 flask.
8. 5 mL of fresh culture medium was added, and the flask was returned to the incubator.
9. The previous flask was discarded as biohazardous waste.

A.3 Seeding Protocol

For imaging experiments, cells were seeded into 35 mm glass-bottom MatTek dishes.

1. Cells were detached and resuspended as described in the subculturing protocol.
2. 50 μ L of cell suspension was transferred into a MatTek dish containing 2 mL prewarmed culture medium.
3. The cells were gently mixed to ensure even distribution across the glass surface.

4. Dishes were incubated at 37°C and 5% CO₂ until imaging.
5. Imaging medium (specific glucose conditions) was exchanged approximately 1 hour prior to imaging experiments (see Appendix B for composition).

Appendix B

Glucose Medium

This appendix contains the full composition of the culture medium used for the glucose conditions, including inorganic salts, amino acids and vitamins. These values were used to prepare the medium for the different experimental conditions. For the low glucose medium, mannitol was used to maintain osmotic balance.

B.1 Glucose Concentrations

Table B.1: Glucose concentrations used for the different culture conditions.

Condition	Glucose concentration (mmol/L)
Baseline (Physiological)	5.5
High glucose	20
Low glucose	0

B.2 Inorganic Salt Composition

Table B.2: Composition of inorganic salts used in the culture medium and their calculated osmolarity contributions.

Ingredient	Amount	Molar weight	Van't Hoff	Osmolarity
CaCl ₂	265	146.0	3	5.44
MgSO ₄	97.67	120.37	2	1.62
KCl	400	74.55	2	10.73
NaHCO ₃	2200	84.00	2	52.37
NaCl	6350	58.44	2	217.32
NaH ₂ PO ₄	122	119.98	2	2.03
Total osmolarity				289.51

B.3 Amino Acid Composition

Table B.3: Amino acid composition of the culture medium.

Ingredient	Amount (mg/L)
L-Arginine Hydrochloride	126
L-Cystine 2HCl	31
L-Glutamine	292
L-Histidine Hydrochloride-H ₂ O	42
L-Isoleucine	52
L-Leucine	52
L-Lysine Hydrochloride	73
L-Methionine	15
L-Phenylalanine	32
L-Threonine	48
L-Tryptophan	10
L-Tyrosine Disodium Salt Dihydrate	52
L-Valine	46
Total osmolarity contribution	4.85 mOsm/L

B.4 Vitamin Composition

Table B.4: Vitamin composition of the culture medium.

Ingredient	Amount (mg/L)
Choline Chloride	1
D-Calcium Pantothenate	1
Folic Acid	1
Niacinamide	1
Pyridoxal Hydrochloride	1
Riboflavin	0.1
Thiamine Hydrochloride	1
Meso-inositol	2
Total osmolarity contribution	0.06 mOsm/L

Appendix C

MSD validation

To evaluate whether the MSD analysis reflected visually observable mitochondrial motion, a time lapse exhibiting temporally varying motility was analysed separately. During manual inspection, mitochondrial movement appeared more pronounced during the early part of the recording, while substantially reduced movement was observed during later frames.

The trajectory data was therefore divided into an early interval (frames 1-90) and a late interval (frames 90-600), and MSD analysis was performed separately for each interval. The resulting MSD curves are shown in Figure C.1.

The early interval showed a steeper MSD curve and a higher α -value compared to the later interval, consistent with the visually observed reduction in mitochondrial movement. This qualitative comparison supports that the MSD analysis captured relative differences in motility within the time lapse.

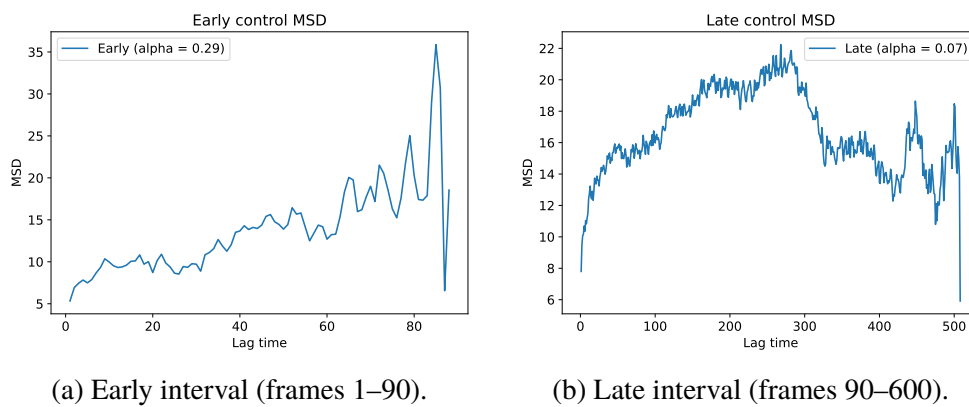


Figure C.1: Qualitative validation of the MSD analysis using a representative time lapse with temporally varying mitochondrial motility. (A) MSD curve calculated from the early interval of the recording, where mitochondria visually exhibited higher motility. (B) MSD curve calculated from the later interval of the recording, where mitochondrial movement appeared substantially reduced.

TRITA-SCI-GRU 2026:072
Stockholm, Sweden 2026

www.kth.se